scientific reports

Check for updates

OPEN

Immune-related hub genes and their role in psoriasis pathogenesis

Tingting Yin, Tingting Zhang✉ & Lei Ma✉

Psoriasis is a prevalent inflammatory skin disorder with immune-related mechanisms that remain incompletely understood. To elucidate the immune landscape of psoriasis, we analyzed expression profiles to identify 115 psoriasis susceptibility genes (PSGs) and subsequently pinpointing eight immune-related hub genes (IRHGs). A predictive model incorporating these IRHGs demonstrated promising prognostic potential for psoriasis. Additionally, extensive intercellular communication was observed among keratinocytes, dendritic cells, monocytes, and T cells. The cellular differentiation trajectory revealed a complex interplay among various cell types and states, highlighting genes such as *CXCL8*, *CCL2*, *STAT3*, and *STAT1* emerging as closely associated with the cellular composition and functional status within the psoriatic immune microenvironment. The present study may shed light on the understanding of the immunopathological dynamics of psoriasis and the development of novel therapeutic strategies and biomarkers for this multifaceted skin disorder.

Keywords Psoriasis, Bulk RNA-Seq, scRNA-Seq, Prognostic model, Immune microenvironment

Psoriasis, a chronic autoimmune disorder, predominantly targets the skin[1], stemming primarily from immune system dysregulation that disrupts some biological equilibria[2]. In the context of psoriasis, immune cells, particularly T cells, along with other pivotal inflammatory players such as macrophages and dendritic cells, undergo heightened activation. This abnormal activation triggers a cascade of inflammatory reactions that contribute significantly to the development and perpetuation of the disease[3–5].

The skin of psoriasis patients is characterized by hyperproliferation of keratinocytes. The life cycle of these cells is shortened, resulting in the accumulation of scaly, immature cells on the skin's surface[6,7]. Additionally, the disease pathology is marked by an amplified inflammatory response and a pervasive immune imbalance[8]. Various factors interact to exacerbate the skin symptoms and the inflammatory progression of psoriasis, highlighting the need for specific immune-related biomarkers that can improve our understanding of the disease and aid in its management. Therefore, identifying these biomarkers is crucial for advancing both our knowledge and the clinical management of psoriasis.

Our aim is to elucidate the immune landscape of psoriasis by analyzing transcriptomic data from psoriatic samples (Fig. 1). We identified 115 psoriasis susceptibility genes (PSGs) and further condensed these to eight immune-related hub genes (IRHGs) to construct a prognostic model for psoriasis. By investigating the roles of these IRHGs and their interactions with various immune cells, we seek to provide new insights into potential biomarkers for psoriasis.

Materials and methods

Data sources

Psoriatic bulk transcriptomic sequencing datasets were downloaded from the GEO database (https://www.ncbi.nlm.nih.gov/geo/), encompassing GSE30999 and GSE201827. The datasets include 217 psoriatic samples and 102 normal samples. We employed the combat package in R to remove batch effects from all expression profiles. Psoriatic trait information from GSE30999[9] and GSE201827[10] were utilized to correlate gene expression with traits. In addition, psoriasis single-cell transcriptomic sequencing dataset GSE151177[11], were downloaded from the GEO database, comprising 13 psoriatic samples and 5 normal samples. Furthermore, the atopic dermatitis (AD) dataset GSE174582, including 30 disease samples and 4 controls, was also obtained. Detailed information regarding all gene expression profiles is delineated in Supplementary Table 1.

Identification of differentially expressed genes in psoriasis

The "limma" package in R was utilized to identify differentially expressed genes. The screening for differentially expressed genes was conducted using thresholds of |log2 fold change (FC)| > 1 and $p < 0.05$, which were then visualized using volcano plots.

College of Life Science, Shihezi University, Shihezi City, Xinjiang, China. ✉email: zting@shzu.edu.cn; malei1979@hotmail.com

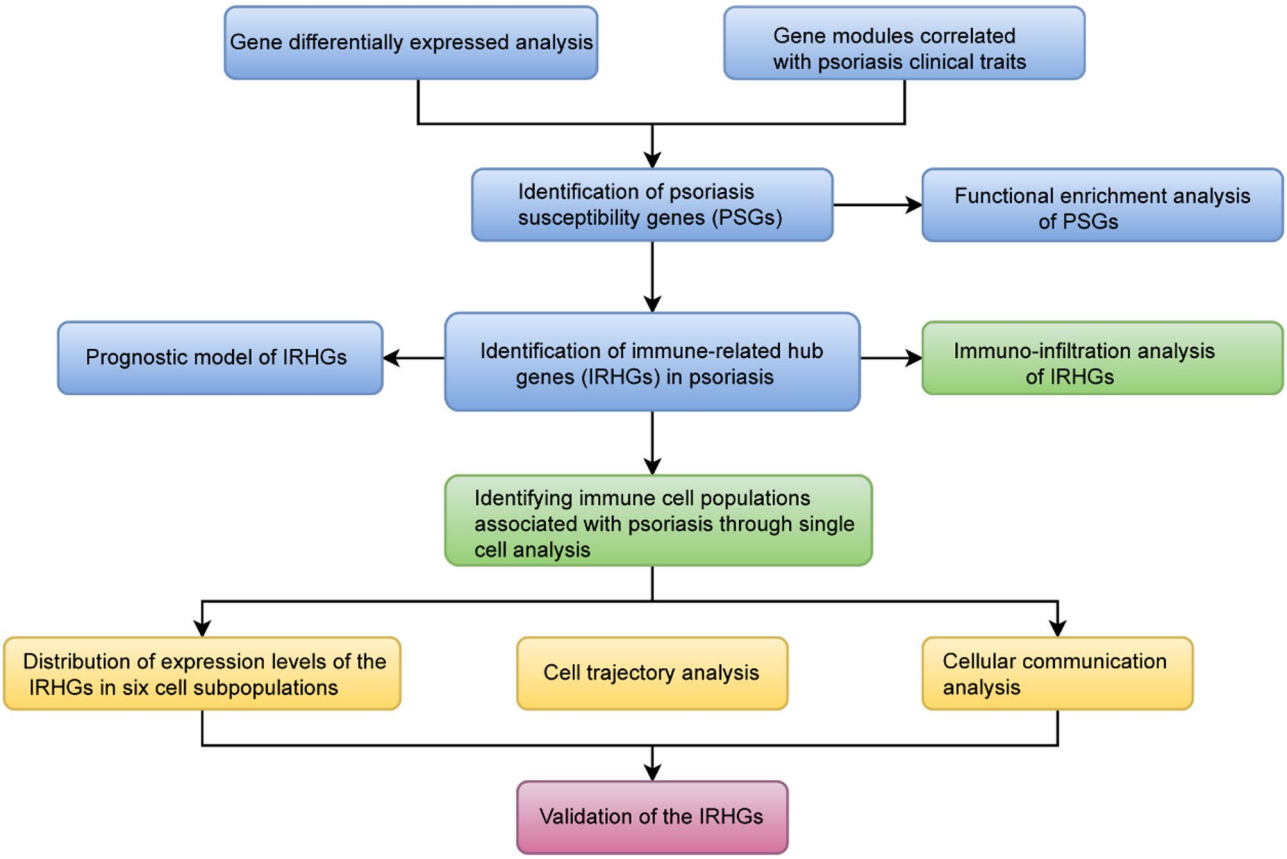

Fig. 1. A framework to delineate the immune landscape.

WGCNA identified key modules associated with psoriasis

The gene networks were constructed using the WGCNA package in R. To ascertain the optimal soft threshold for constructing the adjacency matrix, the scale-free topology criterion was employed, and the "pickSoftThreshold" function was used to select the soft threshold. Through this process, it was determined that the optimal soft threshold β is 14. Next, closely interconnected genes were clustered, module detection was performed using an unsupervised clustering method, and the correlation between modules and genes was calculated. For further validation, module genes with the strongest correlations with psoriasis clinical traits (baseline psoriatic skin lesions) were selected for subsequent analysis.

Functional enrichment analysis

To explore the biological functional categories and potential mechanisms of psoriasis-causing genes, Gene Ontology (GO)[12] and Kyoto Encyclopedia of Genes and Genomes (KEGG) analyses were conducted[13–15].

Identification and modular analysis of IRHGs

The R package 'venn' was used to perform a cross-analysis of the psoriasis-related genes identified by the two methods mentioned above, and the set of psoriasis-associated genes was retrieved from GeneCards (https://www.genecards.org/) to identify the common psoriasis-causing genes. PPI networks from STRING database (https://cn.string-db.org/)[16] and Cytoscape software (version 3.8.1)[17] were used to explore the physical interactions between proteins but also their functional associations. Five distinct topological analysis methods, namely Degree, EPC, MNC, Radiality, and Closeness, were employed to filter out pivotal genes of importance, with the top 10 genes with the highest scores selected from each method. The intersection of the candidate genes obtained from these five algorithms was then taken. Lastly, these candidate genes were analyzed in comparison with known immune genes, leading to the identification of IRHGs.

Construction and evaluation of a nomogram for predictive modeling of diagnostic markers for IRHGs

Receiver operating characteristic curve (ROC) analysis was conducted to evaluate the predictive efficacy of each of the IRHGs genes, and area under the curve (AUC) values were calculated using the "pROC" package. IRHGs with an AUC > 0.8 were considered to possess high potential for psoriasis diagnosis. Utilizing these eight core genes, the "rms" package in R software was employed to construct a nomogram for evaluating each pivotal gene and their performance in psoriasis diagnosis. Calibration curve, Decision Curve Analysis (DCA), and clinical impact curve analyses were performed to assess the efficacy of the nomogram in psoriasis prediction.

Evaluation of immune cell infiltration and its correlation with IRHGs

The relationship between immune infiltrating cells and key biomarkers was investigated based on Spearman correlation using the CIBERSORT tool. The R package "corrplot" was used to visualize the expression matrix of Spearman correlation coefficients among 22 immune cells in the psoriasis dataset. In addition, the correlation between the expression of IRHGs and immune cell infiltration was calculated using the R packages "reshape2", "ggpubr", "ggExtra", and "ggstatsplot", and visualized with the "ggplot2" package.

Drug sensitivity analysis of candidate markers

IRHGs were searched against the Connectivity Map database (https://clue.io) to identify potential small molecule drugs for the treatment of psoriasis. Ultimately, the top 10 compounds with the highest enrichment scores were identified.

Single-cell analysis

We used the "Seurat" package to process single-cell RNA sequencing data. First, cells were filtered with a threshold of min.cells = 3 and min.features = 250, requiring the number of expressed genes detected per cell be between > 500 and < 6000. At the same time, we excluded the top 3% of cells with the highest nCount_RNA expression and the top 2% of cells with the highest mitochondrial gene content. For quality control, we also removed the smallest 1% and the largest 1% of cells based on the proportion of rRNA expression to the total genes in each cell.

Upon completing data preprocessing, the data were normalized using the LogNormalize method. Subsequently, unsupervised clustering was performed, encompassing principal component analysis (PCA) and UMAP analysis[18], enabling the visualization of different cell populations' distribution on a 2D map.

Next, cellular annotation was carried out using the "SingleR" package[19], with reference data sourced from the Human Primary Cell Atlas. For the identification of marker genes for each cell population, the "FindAllMarkers" function was utilized with a fold change (FC) ≥ 1 set as the criterion. This strategy was also employed to screen for differentially expressed genes across different cell populations. Subsequently, the identified marker genes were visualized using the VlnPlot and FeaturePlot functions.

Finally, the Monocle software package was utilized to perform machine learning based on the expression patterns of key genes to simulate dynamic changes during temporal development. The results of cell trajectories should be based on the distribution of trajectories by cell type as well as changes in the expression of characterized genes to confirm the start and end points of differentiation. Upon identifying the cell types in psoriasis, CellChat (version 1.1.3) was employed to analyze intercellular communication.

RNA extraction and qRT-PCR

Total RNA was extracted from the blood samples of one healthy individual and one psoriasis patient using the EasyPure Blood RNA Kit (TransGen Biotech). The extracted RNA was then reverse transcribed into cDNA using the RNA Reverse Transcription Kit (PCR Kit AMV ver. 3.0). Real-time quantitative PCR (RT-qPCR) analysis was performed on the synthesized cDNA using the Roche fluorescence quantitative kit (FastStart Universal SYBR Green Master). Each sample was subjected to three biological replicates. The $2^{-\Delta\Delta CT}$ method was used to calculate and analyze the mRNA expression levels of C-X-C Motif Chemokine Ligand 1 (*CXCL1*), C-X-C Motif Chemokine Ligand 8 (*CXCL8*), C-X-C Motif Chemokine Ligand 10 (*CXCL10*), C-C Motif Chemokine Ligand 2 (*CCL2*), Toll Like Receptor 2 (*TLR2*), Signal Transducer And Activator Of Transcription 1 (*STAT1*), Signal Transducer And Activator Of Transcription 3 (*STAT3*), and Interleukin 1 Beta (*IL1β*), using *GAPDH* as the internal control gene. The sequences of the relevant primers can be found in Supplementary Table 2. The study was conducted in accordance with the Declaration of Helsinki and approved by the Ethics Committee from The First Affiliated Hospital of Shihezi University, China (Approval Number: KJ2024-293-02). Informed consent was obtained from all subjects involved in the study.

Result

Identification of genes associated with psoriasis progression

By comparing transcriptomic data from psoriasis samples with control samples, a total of 1,673 differentially expressed genes were identified. Of these, 680 genes exhibited up-regulation in expression, while 993 genes were down-regulated (Fig. 2a). The down-regulated genes, such as *S100A12*, *TMPRSS11D* and *KYNU*, are mainly involved in cytokine-cytokine receptor interactions, NOD-like receptor signaling, and IL-17 signaling pathways (Supplementary Fig. 1a). Conversely, up-regulated genes, such as *BCAR3*, *JADE1*, and *KRT77*, are mainly involved in the AMPK, Wnt, and PPAR signaling pathways (Supplementary Fig. 1b).

In the gene network of psoriasis samples, we identified 18 expression modules with module sizes ranging from 118 to 2,659 genes. For description and analysis, these modules were labeled with different colors (Fig. 2b, c). Some network modules may play a key role in the biological function of psoriasis. For example, gene expression in the blue module was highly correlated with the baseline of patient skin lesions (Spearman $r = 0.73$). Genes in this module are predominantly associated with biological pathways involved in immune regulation and inflammatory response (Supplementary Fig. 1c).

The set of differentially expressed between the psoriasis group and the control group overlapped with the set of network module genes. For example, there is a set of genes related to immune regulation in the blue network module, and some genes related to immune response in the differential gene set. By combining the genes known to be associated with psoriasis in GeneCards, the differentially expressed genes, and the modular genes, we discerned 115 psoriasis susceptibility genes (PSGs) (Fig. 2d).

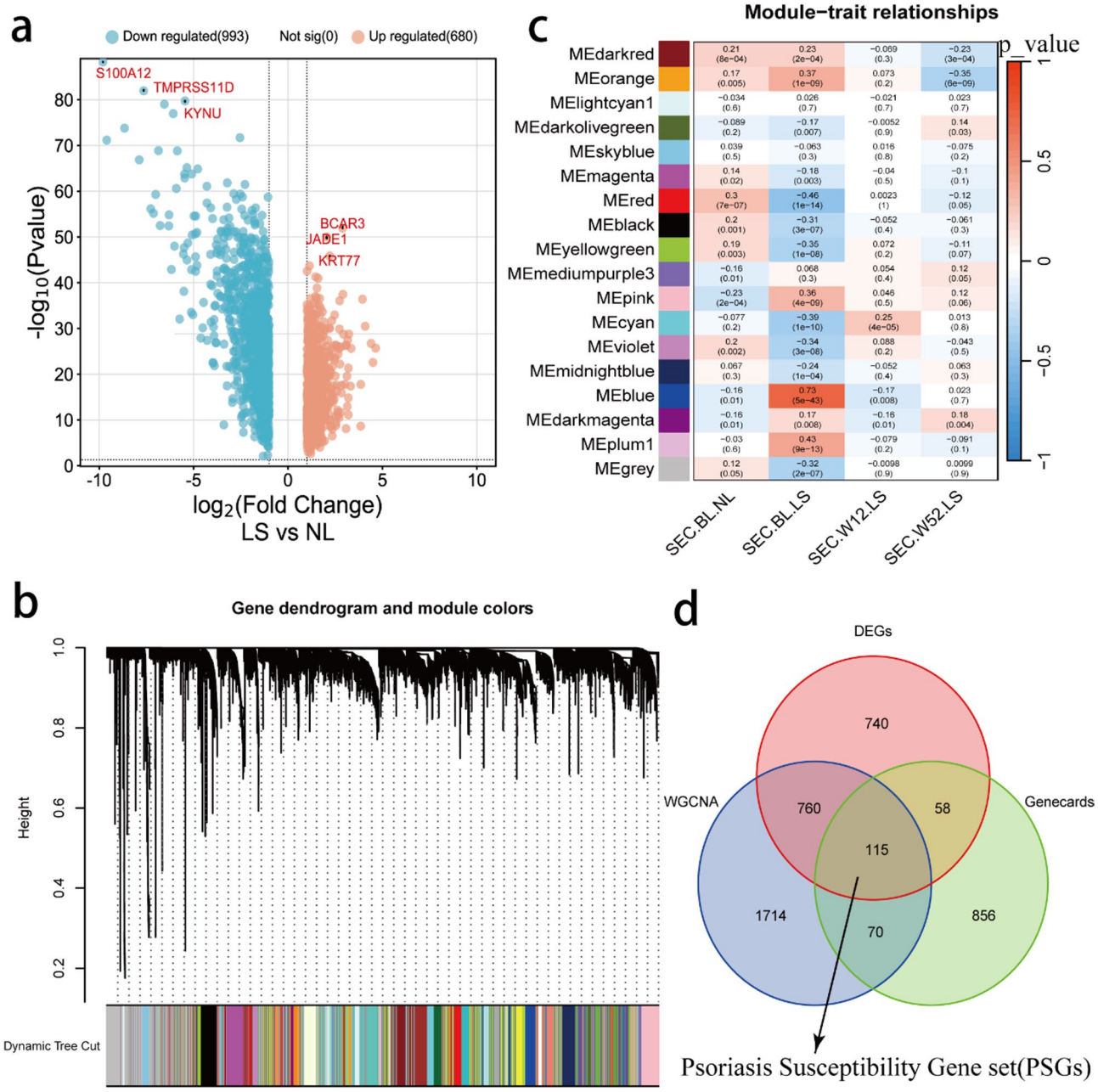

Fig. 2. Identification of psoriasis-related susceptibility genes (PSGs). (**a**) Differential gene expression between the psoriasis group (LS) and the control group (NL). (**b**) Tree diagram of gene expression levels. The upper figure shows the clustering relationship of genes at the transcriptional level, while the lower figure illustrates different clusters denoted by different colors. (**c**) Pearson correlation analysis of the modules (clusters in b) with different psoriasis clinical traits. The horizontal represents the first principal component value of the network module. Vertical axis represents trait data (GSE201827), including psoriasis non-lesion baseline data (SCE.BL.NL), psoriasis lesion baseline data (SCE.BL.LS), Secukinumab-treated psoriasis lesion skin 12-week data (SCE.W12.LS), and 52-week data (SCE.W52.LS). In the heatmap table, the correlation and significance (p_value) between the modules and the different traits of psoriasis are indicated, respectively. (**d**) Intersection among differentially expressed genes (DEGs) from transcriptomic data of psoriasis and control samples, module genes with the strongest psoriasis correlation identified by WGCNA, and genes known to be associated with psoriasis in GeneCards.

Functional enrichment and modular analysis of PSGs

PSGs are primarily involved in a variety of inflammatory responses and immune pathways, encompassing various biological processes such as responses to lipopolysaccharides, cytokine-mediated signaling, granulocyte chemotaxis, and keratinocyte envelope formation. Additionally, these genes play roles in molecular functions related to cytokine activity, receptor-ligand interactions, and signaling receptor activation. Furthermore, they

were associated with multiple KEGG pathways, including cytokine-cytokine receptor interactions, the IL-17 signaling pathway, and the NOD-like receptor signaling pathway (Fig. 3a, b). These findings imply an important role of immune activation and inflammatory pathways in psoriasis progression.

In addition, we calculated the Betweenness centrality index in the gene network of the psoriasis samples and found higher centrality of *IL1β* in the PSGs (Supplementary Fig. 2). *IL1β*, a known cytokine, induces Th17 cell production and promotes keratinocyte chemokine secretion[20]. Its expression is regulated by the nucleotide-binding oligomerization structural domain-like receptor 3 (NLRP3) inflammasome[21], suggesting that *IL1β* may play a key role in immunomodulation in psoriasis.

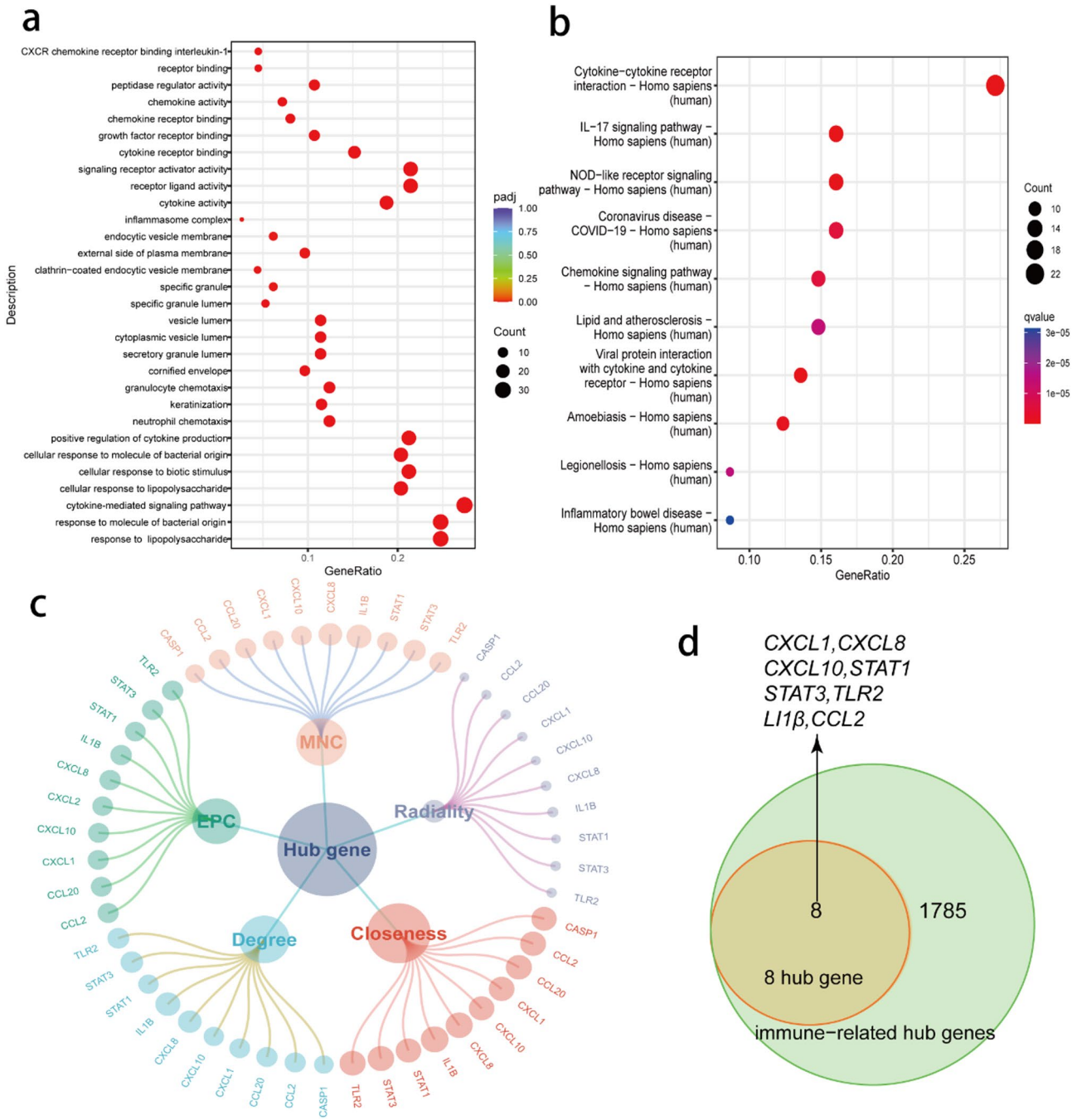

Fig. 3. Functional enrichment and identification of IRHGs. (**a**, **b**). Functional enrichment analysis results in GO (Gene Ontology)[12] and KEGG (Kyoto Encyclopedia of Genes and Genomes)[13–15] of PSGs. (**c**) Identification of IRHGs using centrality indicators from cytoHubba. The outermost circle represents IRHGs, which have high scores in various indicators and are therefore considered to have important centrality or criticality in biological networks. (**d**) IRHGs are immune-related genes.

Identification of IRHGs

Some PSGs in the gene network may play an important role in the development of psoriasis. To explore the role of PSGs in the network, we assessed the network significance of PSGs using five hub metrics (Degree, EPC, MNC, Radiality and Closeness). Among PSGs, eight genes (*CCL2*, *CXCL1*, *CXCL10*, *CXCL8*, *IL1β*, *STAT1*, *STAT3*, and *TLR2*) showed high node centrality across these metrics (Fig. 3c), implying that these PSGs occupy a critical position in the network and may be core targets in psoriasis. Upon searching the Immunology Database, the above eight PSGs were also identified as immune genes. These hub PSGs are thus designated as immune-related hub genes (IRHGs) associated with psoriasis (Fig. 3d).

Evaluation of the diagnostic effectiveness of IRHGs

We constructed a predictive model for psoriasis diagnosis using IRHGs as biomarkers and evaluated the efficacy of IRHGs in psoriasis diagnosis using ROC curves. In the psoriasis dataset (GSE30999), the AUCs of the eight IRHGs (*CCL2*, *CXCL1*, *CXCL10*, *CXCL8*, *IL1β*, *STAT1*, *STAT3*, and *TLR2*) all surpassed 0.8 (Fig. 4a). Moreover, in another independent dataset (GSE201827), the AUC values for all eight IRHGs were all greater than 0.8 (Fig. 4b), indicating that these IRHGs can effectively distinguish psoriatic lesional tissue from healthy skin tissue. To further assess their specificity, we analyzed these IRHGs in psoriasis and atopic dermatitis samples (GSE174582). Six genes (*CCL2*, *CXCL1*, *CXCL10*, *CXCL8*, *STAT1*, and *STAT3*) showed AUC values greater than 0.8, while *TLR2* and *IL1β* demonstrated lower discriminative power (AUC = 0.615 and 0.658, respectively; Supplementary Fig. 3). These results suggest that the six IRHGs (*CCL2*, *CXCL1*, *CXCL10*, *CXCL8*, *STAT1*, and *STAT3*) may serve as psoriasis-specific biomarkers.

In addition, IRHGs exhibited varying levels of expression across different samples of psoriasis. Specifically, IRHGs were significantly up-regulated in skin lesion samples and down-regulation after 12 and 52 weeks of treatment with Secukinumab, suggesting that Secukinumab exerted an inhibitory effect on the expression of IRHGs during the treatment of psoriasis (Fig. 4c).

We utilized a logistic regression model encompassing IRHGs, assigning each gene a score (Points in Fig. 5a) based on its contribution to the outcome variable. Subsequently, the scores of the genes were aggregated to yield the total score (Total Points), from which the risk probability of disease (Risk of Disease) were derived. The outcomes are depicted in the form of a nomogram (Fig. 5a), and a calibration curve was used to assess the predictive efficacy of the model. The calibration curve displays an absolute error of 0.023 between actual and predicted risk, indicating that the logistic regression model is both stable and accurate (Fig. 5b).

The predictive model, using IRHGs as predictive markers, is rational for disease occurrence probabilities between 0 and 0.6. It offers the highest net benefit compared to a strategy that assumes all patients are either positive or negative, with net benefit reflecting the balance between true positives and false positives. However, for disease probabilities greater than 0.6, the net benefit rapidly decreases, approaching the net benefit of a strategy that treats all patients as negative ('None') (Fig. 5c).

In addition, as the high-risk threshold increased, the number of false positives predicted by the model progressively decreased. Both the number of individuals categorized as high risk (represented by the red solid line in Fig. 5d) and the number of high-risk individuals who experienced true events (represented by the blue dashed line in Fig. 5d) gradually declined. However, the rates of these reductions converged over time. This convergence suggests that the model's interpretation positivity rate closely aligns with the true positivity rate at higher risk thresholds.

Identification of immune cell infiltration in psoriasis and its correlation with IRHGs

To explore the immune landscape of psoriasis, we assessed the proportions of 22 immune cell types in both control and psoriasis groups. We found significantly higher proportions of CD4 memory T cells, helper T cells, activated dendritic cells, and M1-type macrophages in psoriasis samples compared to controls (Fig. 6a).

We further evaluated the relationship between IRHGs and immune cells. In the psoriasis dataset, IRHGs were strongly correlated with helper T cells, activated dendritic cells, activated CD4 memory T cells, M1 macrophages, neutrophils, γδ T cells, activated mast cells, and eosinophils. In psoriasis samples, the expression levels of IRHGs were positively correlated with the infiltration of helper T cells, activated dendritic cells, activated CD4 memory T cells, and M1 macrophages; and negatively correlated with the infiltration of regulatory T cells and quiescent mast cells (Fig. 6b).

Identification of potential small molecule compounds for psoriasis treatment

To explore small molecule drugs with potential therapeutic effects for psoriasis, we searched compounds in the Connectivity Map (CMap) database. Some compounds were found to induce the expression pattern of IRHGs in the disease state. By potentially altering the expression patterns of target genes, these compounds may hold therapeutic potential or contribute to the amelioration of psoriasis.

The top 10 compounds identified for their pronounced interference effects include triamcinolone, GDC-0941, selumetinib, MDM2-inhibitor, avrainvillamide-analog-5, tipifarnib, FG-7142, VEGF-receptor-2-kinase-inhibitor-IV, TPCA-1, and benzanthron (Supplementary Fig. 4a, c). Among them, VEGF-receptor-2-kinase-inhibitor-IV is a VEGFR inhibitor (Supplementary Fig. 4b). Levels of VEGF and its receptors are known to correlate with disease severity in the plasma and skin of patients with psoriasis. Furthermore, topical or systemic treatment in psoriasis patients leads to a reduction VEGF levels and vascular proliferation[22,23]. Thus, VEGF-receptor-2-kinase-inhibitor-IV may be a potential small molecule compound for psoriasis treatment.

Identification of psoriasis cell subtypes

We observed variations in the expression levels of IRHGs across different psoriatic cell subpopulations, potentially linking to their underlying pathological mechanisms. Firstly, we filtered 4,789 single-cell transcriptome data

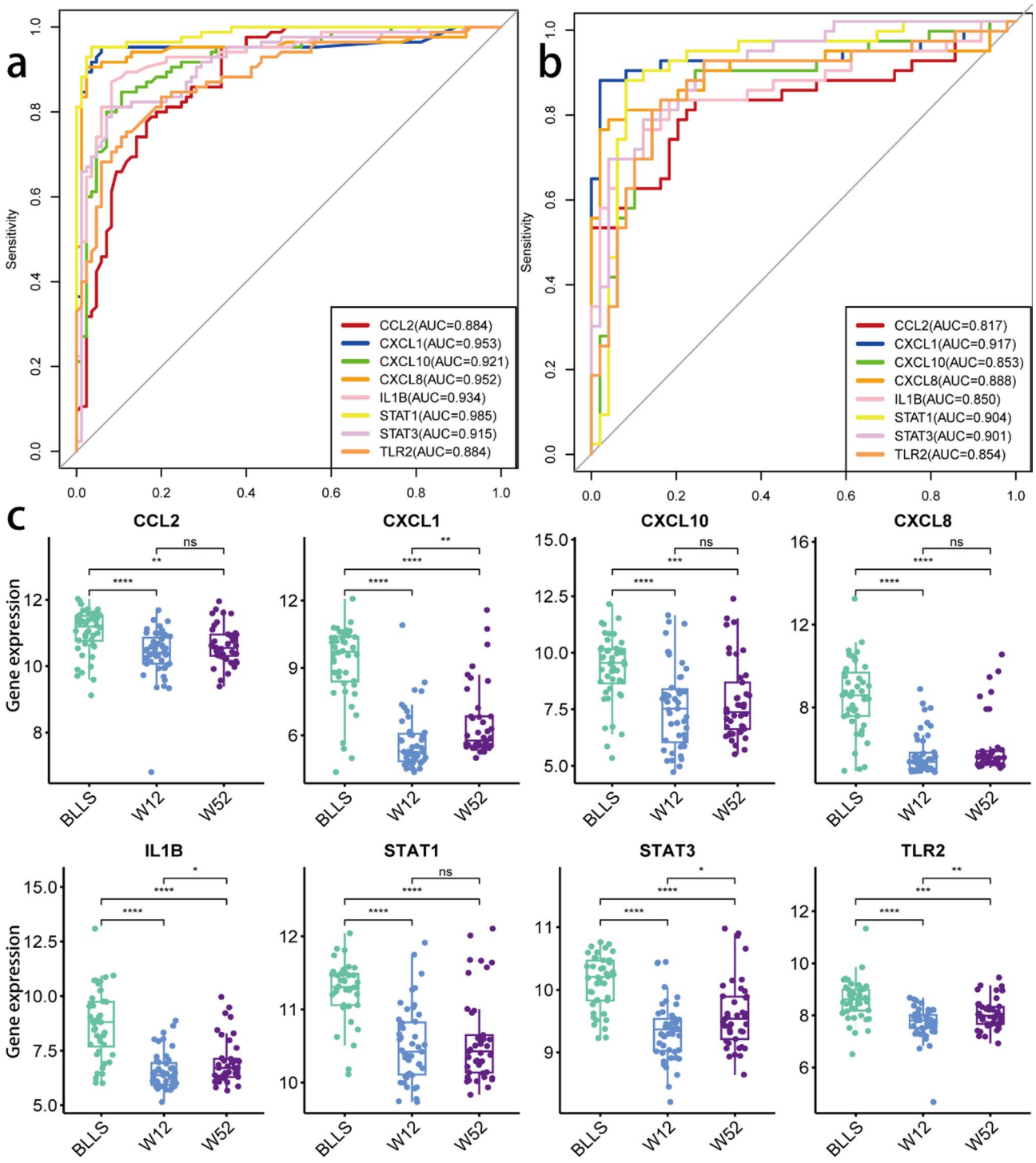

Fig. 4. Validation of IRHGs. (**a**, **b**) ROC curves for a psoriasis diagnostic model using IRHGs as biomarkers. Validation analysis was performed with two independent datasets (GSE30999 and GSE201827), respectively. IRHGs are denoted by different colors. (**c**) Comparative analysis of the expression levels of IRHGs in baseline lesion samples (BLLS), 12-week samples (W12) and 52-week samples (W52) from the psoriasis dataset (GSE201827) was performed using the Wilcoxon rank sum test. The box plot illustrates the distribution of expression level across different samples, showcasing the median, quartiles, and outliers within the data. *, **, ***, and **** represent $P < 0.05$, 0.01, 0.001, and 0.0001, respectively.

from two sets of psoriasis samples and control samples, considering a range of criteria including the count of genes, the number of UMIs in each cell, the percentage of mitochondrial content, and the proportion of rRNA expression to the total gene count. After elimination of low-quality and dead cells, we obtained transcriptome data for 3,644 cells (Supplementary Fig. 5a). Subsequently, we conducted a variance analysis on the gene

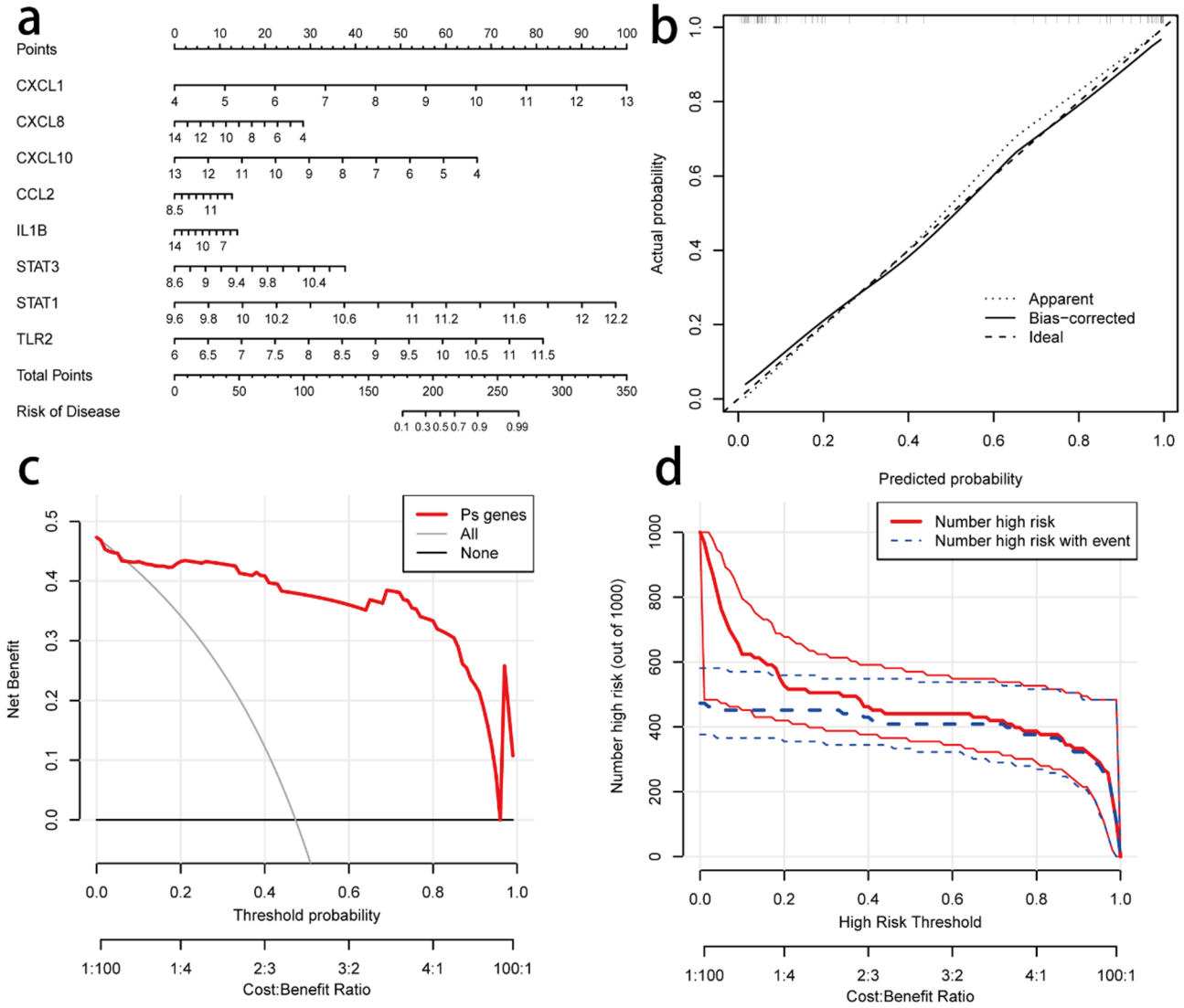

Fig. 5. Evaluation of the diagnostic prediction model. (**a**) Nomogram of Biomarker-based predictive modeling. The lines scale the range of expression levels of the IRHGs, while the length of the line reflects the contribution of IRHGs to the clinical outcome events in psoriasis. The line of 'Points' in the graph represents the contribution scores of IRHGs at different levels; the line of 'Total Points' represents the total score of all IRHGs' contributions; 'Risk of Disease' represents the probability of developing psoriasis. (**b**) Model calibration curves. The thick dotted dashed line, labeled "Ideal", represents the standard curve, showing the perfect prediction of the ideal model. The dotted dashed line, labeled "Apparent", represents the uncalibrated prediction curve, while the solid line, labeled "bias-corrected", represents the calibrated prediction curve. (**c**) DCA (Decision Curve Analysis) of the model. The black line, labeled "none", represents the net gain assuming all patients were negative. The gray line, marked "All", indicates the net benefit assuming all patients are positive. The red line, marked "Ps Genes", indicates the net gain in identifying psoriasis based on the diagnostic value predicted by the nomogram model. (**d**) The clinical impact curves. The solid red curves (Number high risk, with the three solid red lines represent the relevant data at different levels of risk) indicate the number of people classified as positive (high risk) by the model at each threshold probability. The blue dashed curve (Number high risk with event) is the number of true positives at each threshold probability.

abundance in these transcriptome data, identifying the top 2,000 genes with the most significant fluctuations (Supplementary Fig. 5b). We discovered that the top 20 principal components could distinguish these single-cell samples (Supplementary Fig. 5c).

Following this, we performed a cluster analysis of the core cells, categorizing them into six distinct cell clusters and identifying the top five important marker genes for each cell type (Supplementary Fig. 6). We then annotated these cell clusters, identifying six cell groups including keratinocytes, T cells, dendritic cells, and monocytes. Notably, T cells, dendritic cells, monocytes, and IL-22-expressing keratinocytes were present in high numbers in the psoriasis samples (Fig. 7a, b), implying a significant role of these cell populations in the pathogenesis of psoriasis.

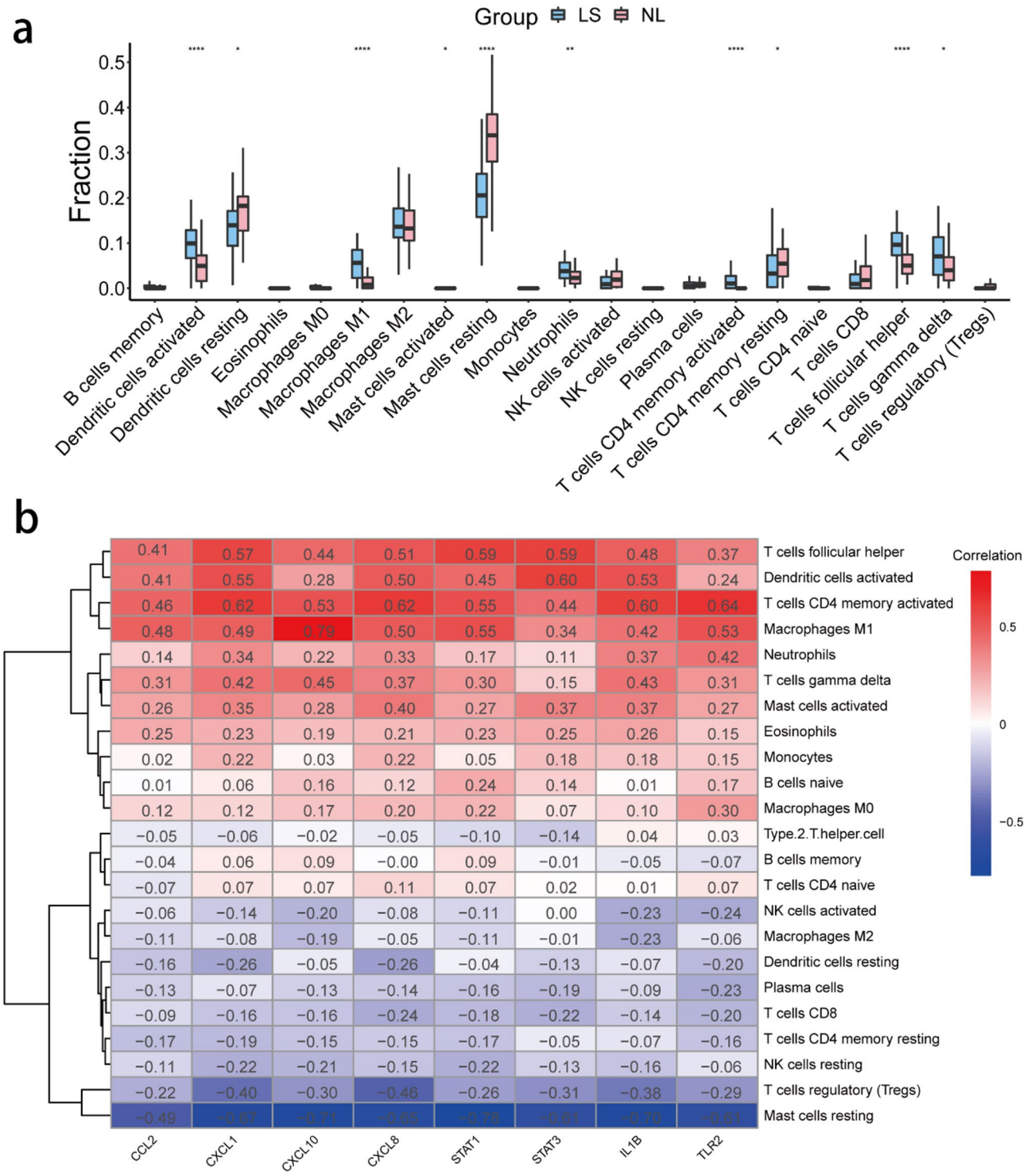

Fig. 6. Immuno-infiltration analysis of IRHGs. (**a**) Differences in immune cell ratios between the control (NL) and psoriasis (LS) groups were compared between subgroups using the Wilcoxon rank sum test. The horizontal axis represents 22 immune cells, while the vertical axis indicates the fraction of a particular type of immune cell in psoriasis samples (blue) and control samples (pink). *, **, ***, and **** indicate $P < 0.05$, 0.01, 0.001, and 0.0001, respectively, while ns indicates $P > 0.05$. The box plot illustrates the distribution of the fraction across different cells, showing the median, quartiles, and outliers within the data. (**b**) Spearman correlation of IRHGs (heat map rows) with infiltrating immune cells (columns).

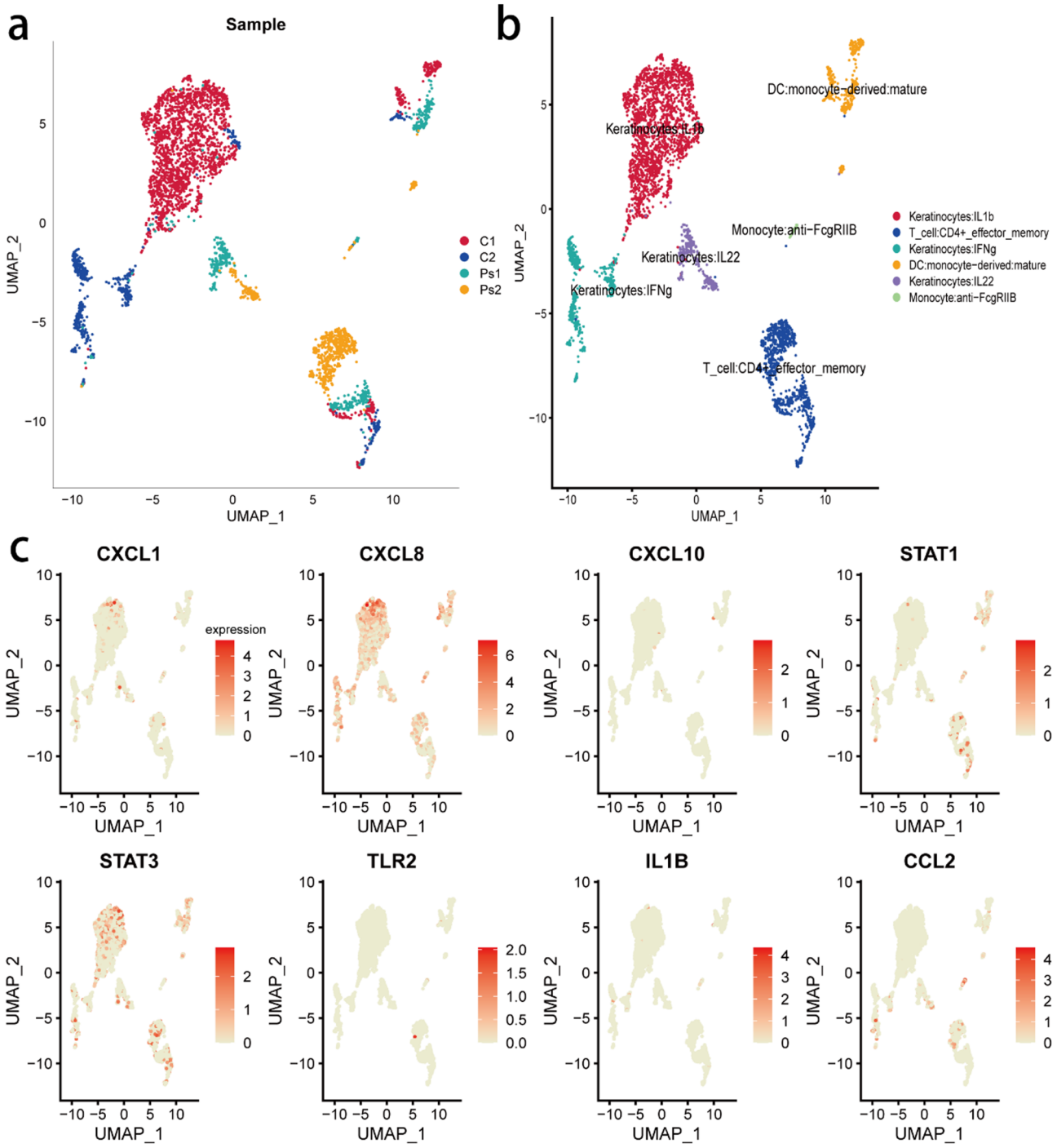

Fig. 7. Cell Clusters. (**a**) Distribution of different cell populations in psoriasis samples (Ps1, 2) and control samples (C1, 2). The horizontal axis (UMAP_1) represents the first principal feature of the data in the reduced low-dimensional space, and the vertical axis (UMAP_2) represents the second principal feature of the data in the reduced low-dimensional space. (**b**) Cell type annotations for clusters. Six cell clusters were annotated as six cell types based on marker genes. (**c**) Distribution of expression levels of the IRHGs in six cell subpopulations.

In addition, we explored the relationship between IRHGs and the six cell populations described above. The results showed that *CXCL8* was highly expressed across all six cell subpopulations (Fig. 7c), suggesting that *CXCL8* may play a role in psoriasis development within these cellular frameworks. On the other hand, *CCL2*, identified as a marker gene, exhibited high expression exclusively in monocytes. We also observed that *STAT1* was highly expressed in monocytes, while *STAT3* was predominantly expressed in IL1β-expressing keratinocytes[24]. Both genes also had relatively high expression levels in dendritic cells. Therefore, we propose

that *STAT3* and *STAT1* may play roles in mediating the inflammatory response, potentially through modulating chemokine expression that facilitates dendritic cell recruitment[25–27].

However, the expression levels of *CXCL1*, *CXCL10*, *IL1β* and *TLR2* are relatively low in these six cell subpopulations. These findings elucidate the expression patterns of IRHGs across different cell subpopulations, suggesting their potential association with psoriasis.

Reconstruction of differentiation trajectories for psoriasis-associated cell subpopulations and analysis of cellular communication

Utilizing psoriasis-associated keratinocytes and T cells, we constructed differentiation trajectories to analyze immune cell heterogeneity among patients (Fig. 8). In this trajectory, keratinocytes, and T cells occupy different branches, each resenting different states of differentiation. Further analysis revealed that effector memory CD4 + T cells progressed toward an IL-22-expressing keratinocyte state before differentiation (bifurcation) occurred. IL-22, produced by CD4 + T cells, is an important downstream cytokine of IL-23. Its receptor IL-22R can be expressed in non-hematopoietic cells like keratinocytes and epithelial cells[28]. Shortly after forming the IL-22-expressing keratinocyte state, the cells bifurcated into two distinct branches, representing the two main cell lineages in the later stages of reprogramming (Fig. 8).

Furthermore, based on the distribution of various cell types under different states, we found that the cell types in State 1 primarily included IL-22-expressing keratinocytes, T cells, and a small proportion of monocytes.

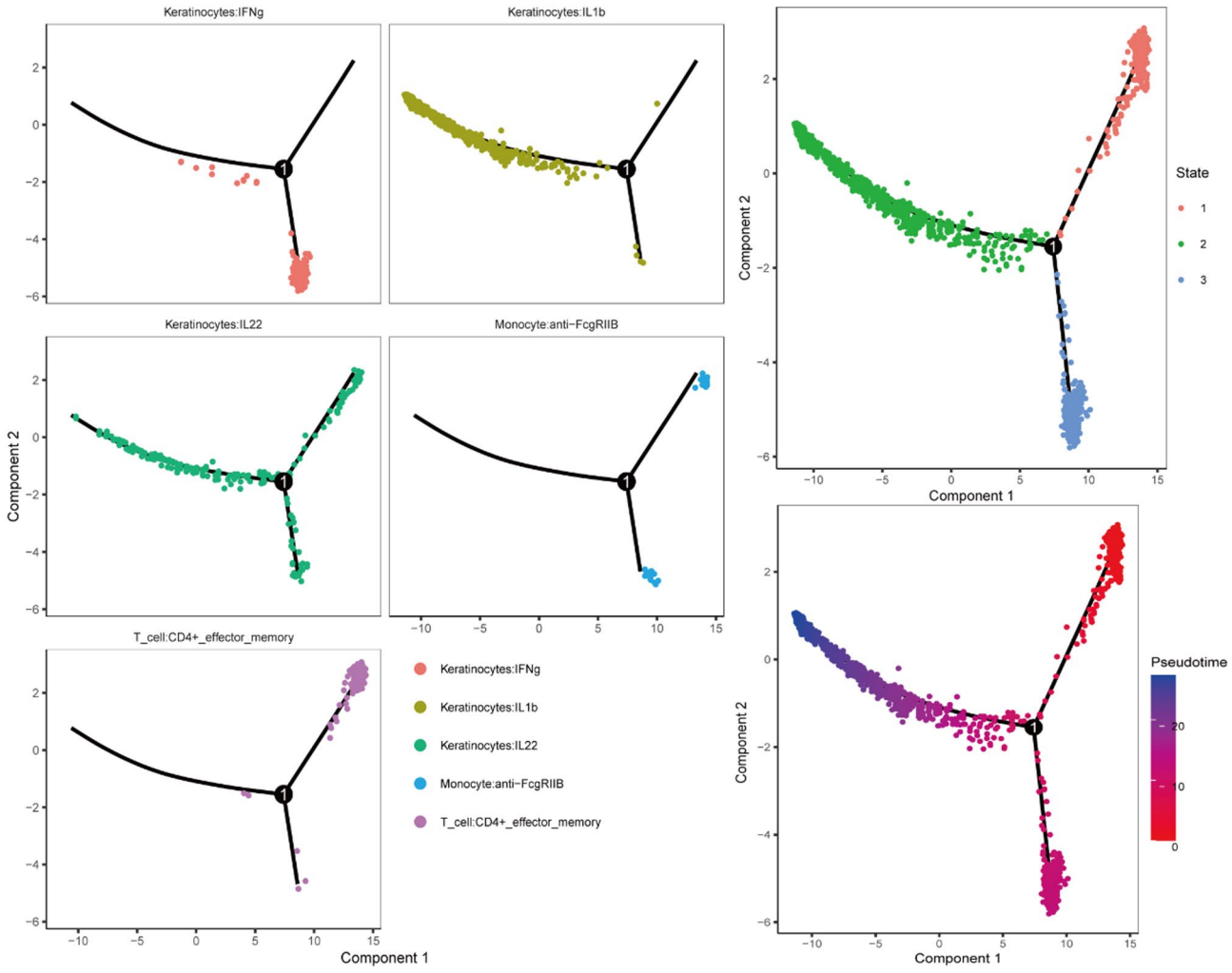

Fig. 8. Cell trajectory analysis. Trajectory analysis revealed five subpopulations of psoriatic cells exhibiting distinct differentiation patterns. One branch evolved into a subset predominantly characterized by IL1β-expressing keratinocytes, while the other branch was dominated by IFN-γ-expressing keratinocytes. The left five panels depict the trajectory differentiation process of different cell subpopulations, with distinct colors representing various immune cells. The upper right panel illustrates three states of cells during trajectory differentiation, each represented by a different color. The lower right panel delineates the pseudotime of cell track differentiation, arranging cells in chronological order of their differentiation or development based on the information gleaned from the single-cell data. The color gradations in the graph indicate the extent of differentiation time.

In State 2, the predominant cell types were IL1β-expressing keratinocytes, T cells, and a few IFN-γ-expressing keratinocytes. State 3 mainly comprised T cells, IFN- γ-expressing Keratinocytes, and a small number of monocytes. In addition, we observed that *CCL2*, *CXCL8*, *STAT3*, and *STAT1* are differentially expressed from State 1 to State 3, suggesting that these genes may serve as markers during the differentiation trajectories of these cells (Supplementary Fig. 7).

We conducted intercellular communication network analysis to predict interactions among six cell subpopulations based on specific ligand receptors. For example, by comparing paired receptors between different cells, we identified interactions between monocytes and keratinocytes expressing IL-22 and IFN-γ (Fig. 9b). In addition, based on differences in the strength of ligand receptor action, we observed a more prominent interaction between dendritic cells and IL-22-expressing keratinocytes. However, there is less interaction between IL1β-expressing keratinocytes and other cells (Fig. 9a). These results are consistent with previous studies and underscore the importance of interactions between keratinocytes and other immune cells in the development of psoriatic lesions[26].

Additionally, we observed several signaling pathways between these six cell subpopulations, including MIF, CD99, CLEC and CCL signaling pathways. In the MIF signaling pathway, we identified two ligand-receptor pairs with significant contributions: MIF-(CD74 + CD44) and MIF-(CD74 + CXCR4) (Fig. 9c). Monocytes secrete MIF, which binds to its receptor CD74 on macrophages, leading to the recruitment of inflammatory factors[29–31]. This interaction results in substantial expression of inflammatory factors such as TNF-γ and IL-22 by keratinocytes in patients with psoriasis, contributing to the dysregulation of the immune homeostasis and the inflammatory response (Fig. 9d, e).

qRT-PCR verification of IRHG expression

To preliminarily validate the expression levels of IRHGs, we performed qRT-PCR analysis on the control and psoriasis groups (Fig. 10). The results indicated that the expression levels of *CXCL1*, *CXCL8*, *CXCL10*, *IL1β*, *STAT1*, and *STAT3* were higher in the psoriasis group compared to the control group, which is consistent with the results from the previous analysis (Fig. 4c).

Discussion

IRHGs interact with immune cells to promote psoriasis development

Psoriasis is a chronic autoimmune skin disease characterized by immune system dysregulation leading to abnormal biological responses[1,2]. During this process, both T cells and inflammatory cells exhibit enhanced activity, releasing inflammatory mediators such as tumor necrosis factor-α and interferon-γ. These mediators, in turn, stimulate abnormal skin cell growth and inflammatory responses[32]. These interactions drive the progression of the skin symptoms and inflammation in psoriasis. Despite the key role of the immune system in the disease, research on immune-related biomarkers in psoriasis remains limited. In-depth studies of these markers and their relationship with immune cells are crucial for diagnosis, treatment, disease assessment, individualized therapy, and clinical trial design. Such research will offer valuable insight into psoriasis research and treatment. In the present study, we employed a fusion of differential expression analysis and WGCNA to identify psoriasis immune-related biomarkers. This approach identified 115 psoriasis susceptibility genes (PSGs) and subsequently aggregated them into eight immune-related hub genes (IRHGs) within the network.

Functional analysis revealed that PSGs are enriched in cytokine-cytokine receptor interactions and the IL-17 signaling pathway, both of which may significantly correlate with the development of psoriasis. Past research has demonstrated that IL-17 plays a key role in psoriasis by triggering the secretion of three different classes of cytokines, each contributing to various stages of the disease[33]. Initially, IL-17 C and IL-36, as class I cytokines, enhance tissue inflammation, thereby advancing the pathological process of psoriasis[34]. Subsequently, induced jointly by TNF-α and IL-17, has the potential to directly cause structural and functional changes in the psoriatic epidermis, thereby intensifying disease severity[35]. Finally, IL-19, a member of the third class of cytokines, amplifies the effects of IL-17 through positive feedback regulation, further facilitating the progression of psoriasis[36].

After identifying a set of PSGs, we aggregated eight IRHGs within network: *CCL2*, *CXCL1*, *CXCL10*, *CXCL8*, *IL1β*, *STAT1*, *STAT3*, and *TLR2*. Using these IRHGs, we constructed a predictive model which exhibited strong performance in ROC curve analysis. The verification through ROC analysis and the expression evaluations confirmed the high prognostic reliability of these IRHGs. Further examinations, using a column-line graphs, calibration curves, and clinical impact curves, highlighted the prognostic significance of these IRHGs for psoriasis patients.

Previously studies have reported that three of the identified immune-related hub genes IRHGs—*CXCL1*, *CXCL8*, and *CXCL10*—are upregulated in psoriatic skin lesions[37,38], with a noted positive correlation between their expression and neutrophil infiltration. This highlights the significance of these genes in the immunopathological progression of psoriasis. Specifically, *CXCL1* and *CXCL8* are chemokines whose expression in keratinocytes is induced by IL-36G, promoting neutrophil migration and contributing to the inflammation characteristic of psoriasis[39]. This aligns with our study outcomes, highlighting the crucial role which these genes play in the psoriatic immune response. Moreover, *CXCL10* functions as a chemokine that attracts immune cells like T cells, monocytes, and NK cells to sites of inflammation. Elevated *CXCL10* expression in psoriasis is associated with immune response and inflammation, potentially leading to an accumulation of immune cells in psoriatic skin and thereby intensifying the inflammatory reaction[40].

CCL2 may play an important role in the pathological development of psoriasis. Our study found elevated expression levels of *CCL2* in psoriasis samples, which were positively correlated with CD4 + T cell infiltration. This finding aligns with other studies that have observed increased *CCL2* expression in the epidermal tissues of

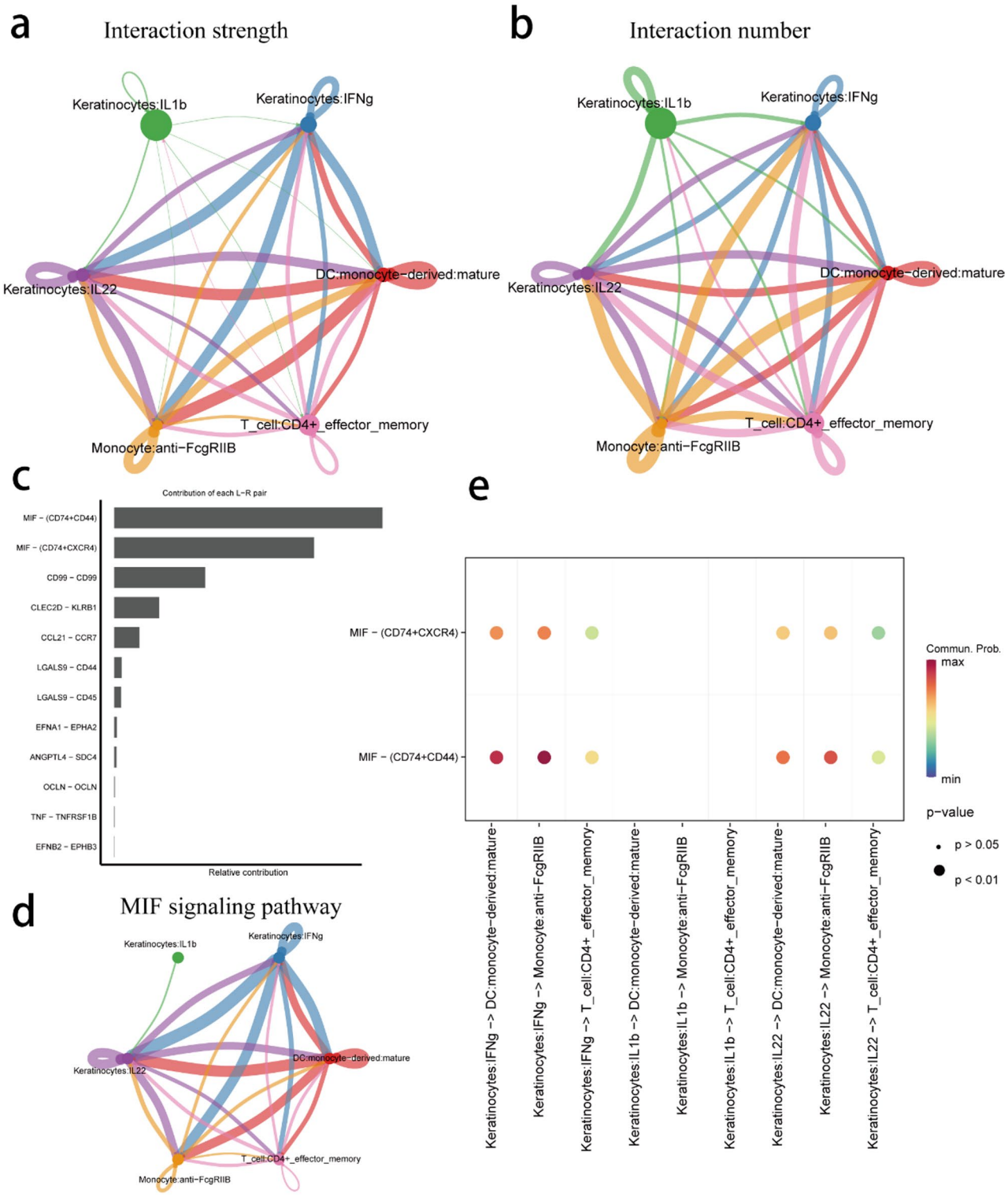

Fig. 9. Cellular communication analysis of six subpopulations of psoriatic cells with different differentiation patterns. (**a**, **b**) Strength and number of interactions between key cells. The wider the line, the stronger and more numerous the interactions. (**c**) The ligand-receptor pair (vertical axis) with the strongest contribution (horizontal axis) in the MIF signaling pathway. (**d**) Interaction of ligand-receptor pairs in the MIF signaling pathway in six different cellular subpopulations. (**e**) Correlation of ligand-receptor pairs in the MIF signaling pathway in different cell subpopulations. Cumulative probability (Commun. Prob) is used to indicate the likelihood of interaction between a particular cell or receptor pair and an immune cell, while the p-value tests whether the interaction between two cell types or receptor pairs has a statistically significant probability value.

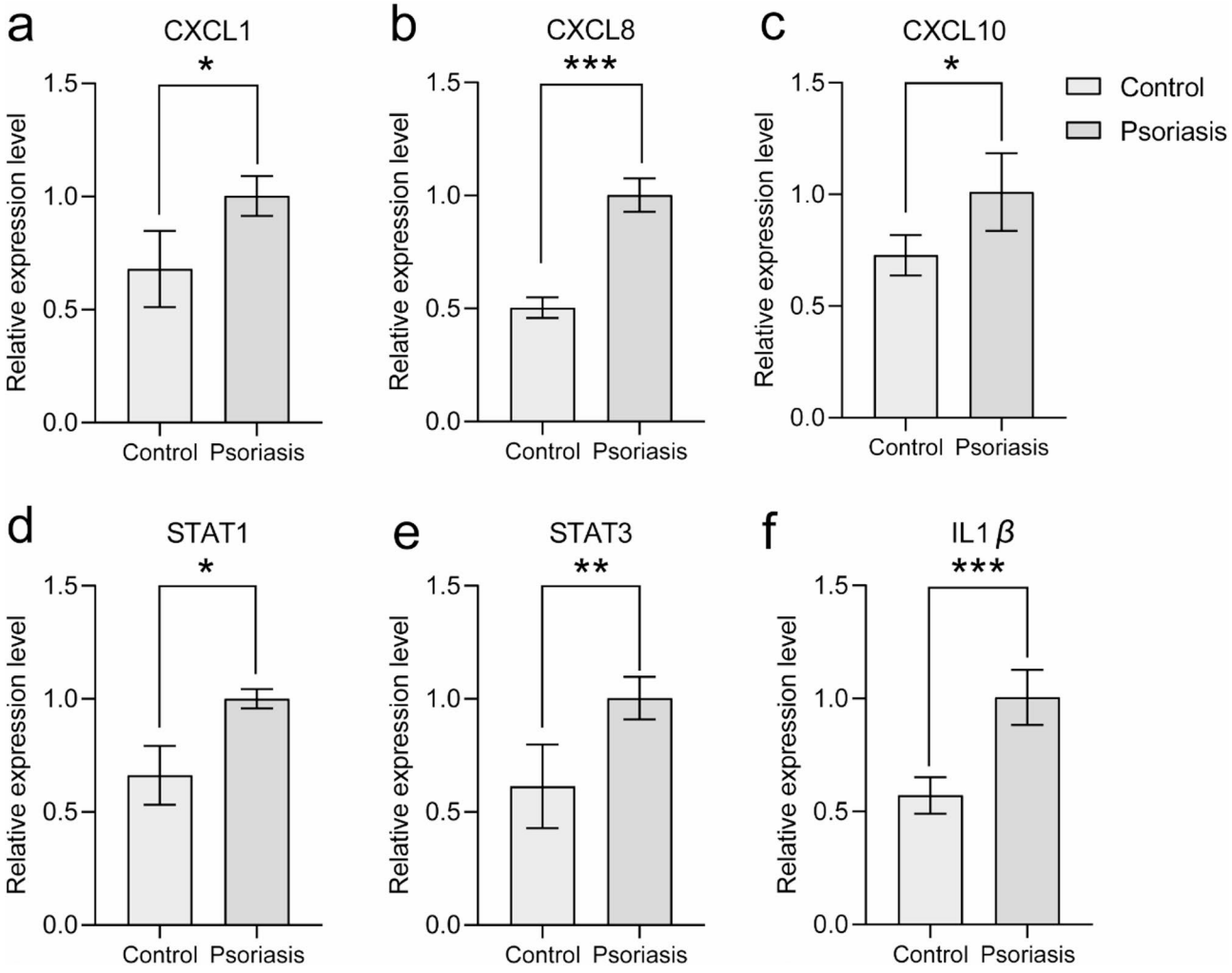

Fig. 10. qRT-PCR validation of the expression in psoriasis of: (**a**) *CXCL1*, (**b**) *CXCL8*, (**c**) *CXCL10*, (**d**) *STAT1*, (**e**) *STAT3*, (**f**) *IL1β*; $^{*}P<0.05$, $^{**}P<0.01$, $^{***}P<0.001$.

psoriasis patients[41]. Such evidence underscores the importance of *CCL2* in the immunopathological dynamics of psoriasis, particularly its association with CD4 + T cell infiltration.

The interplay between *STAT3* and *STAT1* may be crucial in the pathogenesis and progression of psoriasis. In this study, we observed significantly elevated expression levels of both *STAT3* and *STAT1* in psoriasis samples, consistent with previous research showing increased activation of transcription factor *STAT3* in psoriatic skin lesions[42]. Interestingly, when *STAT1* expression was subdued, it disrupted the balance between *STAT1* and *STAT2* activation, shifting the activation state of IL-27 from inhibitory to one that promotes IL-17 A expression[43]. This suggests that heightened *STAT3* activation may enhance pro-inflammatory effects of IL-27 within specific psoriatic immune microenvironments, particularly when the *STAT3*/*STAT1* activation ratio is elevated.

Toll-like receptor 2 (*TLR2*) may play an important role in the innate immune response. In our investigation, we observed a positive correlation between *TLR2* expression and dendritic cell infiltration through immune-infiltration analysis. The *TLR2*-mediated signaling pathway promotes IL-10 production, which is induced by dendritic cells and regulatory T cells[44]. Furthermore, *TLR2* supports the proliferation of regulatory T cells while reducing the release of inflammatory cytokines, thereby significantly alleviating imiquimod-induced skin inflammation in psoriasis[45].

IL-1β plays multiple roles in the context of psoriasis. In our investigation, we observed an elevated expression of *IL-1β* in psoriasis samples, which positively correlated with the infiltration of various T-cell types. *IL-1β* is a potent inflammatory mediator that initiates and amplifies inflammatory responses. Particularly in psoriasis patients, *IL-1β* levels increase, especially within lesion areas[20,46]. *IL-1β* activates inflammatory cells and triggers the release of inflammatory mediators through engagement with its receptor, inducing a localized inflammatory cascade[46]. Additionally, *IL-1β* orchestrates the activity of immune cells, including T cells and inflammatory cells, and plays a crucial role in the migration and aggregation—key aspects in the development of psoriatic skin lesions[47]. *IL-1β* often collaborates with other inflammatory agents, such as tumor necrosis factor-α (TNF-α), to further drive inflammatory reactions and lesion formation, potentially exacerbating the inflammatory condition in psoriatic skin.

Combined analysis of IRHGs and psoriasis-associated cell subsets

Through psoriatic single-cell RNA sequencing (scRNA-seq) profiling, we identified six cell types including keratinocytes, dendritic cells, monocytes, and T cells, which frequently engage in mutual communication. We discovered variations in the expression levels of IRHGs across cell subpopulations, potentially linked to their underlying pathological mechanisms.

CXCL8 exhibited expression across all six cell types, albeit to varying degrees, with a notable expression in keratinocytes. Previous research indicated that *CXCL8*, predominantly produced by keratinocytes, shows heightened expression in psoriatic lesion skin[40]. It induces skin inflammation through interaction with the CXCR1 receptor, guiding neutrophil infiltration into the epidermis. Additionally, while granulocytes and T lymphocytes are dominant players in psoriasis progression, monocytes also hold a crucial role in skin inflammation.

CCL2 is prominently expressed in these cells, serving as a marker gene for monocytes. Research has demonstrated that this molecule coordinates the recruitment of monocytes to inflammation sites via the CCL2/CCR2 signaling pathway, initiating a cascade of inflammatory responses[48,49]. This cascade contributes to the exacerbation of psoriasis, aligning with the observations in our study.

Macrophage migration inhibitory factor (MIF) drives the pathological progression of psoriasis through cross-cell subgroup signaling networks, with mechanisms involving immune regulation, epidermal homeostasis imbalance, and other factors. Studies have found that the abnormal activation of the MIF signaling pathway in monocytes, dendritic cells, and keratinocytes is closely associated with immune dysregulation in psoriasis. Specifically, MIF secreted by T lymphocytes and monocytes targets CD74 receptors and chemokine receptors CXCR2/CXCR4[50], promoting the migration and infiltration of neutrophils and monocytes to the epidermal-dermal junction, thereby participating in the remodeling of the inflammatory microenvironment. Additionally, the binding of MIF to membrane receptor complexes (such as CXCR4/CD74 and CD74/CD44) activates the nuclear factor-kappa B (NF-κB) signaling pathway[30,51], which induces the excessive secretion of pro-inflammatory cytokines such as tumor necrosis factor-alpha (TNF-α) and interleukin-6 (IL-6), further promoting the differentiation of T-helper 17 (Th17) cells and the production of interleukin-17 A (IL-17 A), thereby exacerbating the abnormal activation of the IL-23/Th17 immune axis. In keratinocytes[31,52], MIF activates extracellular signal-regulated kinase (ERK) and phosphoinositide 3-kinase/protein kinase B (PI3K/AKT) pathways[53], stimulating abnormal cell proliferation and inhibiting apoptosis, leading to histopathological changes such as acanthosis and hyperkeratosis. Our findings are consistent with these earlier studies, further validating the important role of MIF in regulating immune and inflammatory responses across different cell subgroups.

This study integrated single-cell transcriptomic data with pseudotime analysis to elucidate the dynamic interaction mechanisms between immune cells and keratinocytes during the pathogenesis of psoriasis. Specifically, CD4 + effector memory T cells follow a clear differentiation trajectory along pseudotime: from a resting state (State1), through an intermediate state (State2), to a terminal activation state (State3). This differentiation process is accompanied by characteristic gene expression changes: early (State1→2), *STAT1* is significantly upregulated, driving Th1-type immune responses; while in the late stage (State3), *STAT3* maintains high expression, promoting the activation of the Th17 pathway[54]. Keratinocytes show dynamic responses to changes in the immune microenvironment, particularly under the stimulation of IFNγ and *IL-1β*, where they actively participate in immune cell recruitment by secreting chemokines such as *CCL2* and *CXCL8*[55]. Notably, *CXCL8* exhibits explosive expression in State2, coinciding with the peak of T cell activation; whereas the activation of *TLR2* in State3 suggests that microbial signals may play a role in maintaining the chronic phase of psoriasis[56]. These findings establish a pathological feedback loop framework of "chemokine recruitment–immune cell activation–epidermal proliferation," providing a single-cell level theoretical basis for the development of stage-specific targeted therapeutic strategies.

This study has certain limitations. First, although preliminary testing of PBMCs showed that the expression trends of the eight IRHGs were consistent with bioinformatics predictions, these results require validation in larger skin tissue samples to establish their reliability as psoriasis biomarkers. Second, while the current sample size ($n = 1$/group) does not meet statistical power requirements, it provides directional insights that can guide future research.

Conclusion

The presented study unveils eight IRHGs and explores their prognostic relevance in psoriasis through comprehensive analysis. Employing scRNA-seq profiling, we deciphered a variety of cell subpopulations and their interactions within the psoriatic immune microenvironment. We found that the expression profiles of these IRHGs varied across different cell subpopulations, highlighting potential ties to the underlying pathological mechanisms of psoriasis. Extensive intercellular communication was observed among keratinocytes, dendritic cells, monocytes, and T cells. The cellular differentiation trajectory in psoriasis revealed a complex interplay among various cell types and states. Moreover, certain genes like *CXCL8*, *CCL2*, *STAT3*, and *STAT1* are closely intertwined with the cellular composition and functional status within the psoriasis immune microenvironment. Through this work, we have garnered a deeper understanding of the immunopathological mechanisms of psoriasis potentially providing valuable insight for the development of future therapeutic strategies and biomarkers for this complex skin disorder.

Data availability

The datasets supporting the conclusions of this articleare available in the Gene Expression Omnibus repository (https://www.ncbi.nlm.nih.gov/geo/).

GSE30999:https://www.ncbi.nlm.nih.gov/geo/query/acc.cgi?acc=GSE30999

GSE201827:https://www.ncbi.nlm.nih.gov/geo/query/acc.cgi?acc=GSE201827

GSE151177:https://www.ncbi.nlm.nih.gov/geo/query/acc.cgi?acc=GSE151177
GSE174582:https://www.ncbi.nlm.nih.gov/geo/query/acc.cgi?acc=GSE174582

Received: 12 November 2024; Accepted: 16 May 2025
Published online: 22 May 2025

References

1. Symmons, D. P. M. et al. Global epidemiology of psoriasis: A systematic review of incidence and prevalence.
2. Grän, F., Kerstan, A., Serfling, E., Goebeler, M. & Muhammad, K. Current developments in the immunology of psoriasis. *Yale J. Biol. Med.* **93** (1), 97–110 (2020).
3. Krueger, J. G., Harden, Jamie, L. & Bowcock, Anne, M. The immunogenetics of psoriasis: A comprehensive review. *J. Autoimmun.* (2015).
4. Diallo, M. Psoriasis Epidemiology. Journal of Clinical Case Reports. ;02(08). (2012).
5. Gayathri, K., Perera, Paola, Meglio, D. & Frank, O. Nestle. Psoriasis. Annual review of pathology. (2012).
6. Owen, C. M., Chalmers, R. J., O'Sullivan, T. & Griffiths, C. E. Antistreptococcal interventions for guttate and chronic plaque psoriasis. *Cochrane Database Syst. Reviews*. **2** (2), CD001976 (2000).
7. MP, S., Boehncke, W. H. & Psoriasis *N. Y. State J. Med.* ;**57**(16):2703. (2005).
8. Muhr, P., Zeitvogel, J., Heitland, I., Werfel, T. & Wittmann, M. Expression of Interleukin (IL)-1 family members upon stimulation with IL-17 differs in keratinocytes derived from patients with psoriasis and healthy donors. *Br. J. Dermatol.* **165** (1), 189–193 (2011).
9. Suárez-Farias, M., Li, K., Fuentes-Duculan, J., Hayden, K. & Krueger, J. G. Expanding the psoriasis disease profile: Interrogation of the skin and serum of patients with Moderate-to-Severe psoriasis. *J. Invest. Dermatology*. **132** (11), 2552–2564 (2012).
10. Blauvelt, A. et al. Psoriasis improvements and inflammatory biomarker normalization with Secukinumab: The randomized ObePso-S study. *J. Dermatol. Sci.* **109** (1), 12–21 (2023).
11. Kim, J. et al. Single-cell transcriptomics applied to emigrating cells from psoriasis elucidate pathogenic versus regulatory immune cell subsets. *J. Allergy Clin. Immunol.* **148** (5), 1281–1292 (2021).
12. Wencke, W., Fátima, S-C. & Mercedes, R. GOplot: an R package for visually combining expression data with functional analysis. *Bioinformatics* (17):2912–2914. (2015).
13. Kanehisa, M., Furumichi, M., Sato, Y., Matsuura, Y. & Ishiguro-Watanabe, M. KEGG: biological systems database as a model of the real world. *Nucleic Acids Res.* **53** (D1), D672–D7 (2025).
14. Kanehisa, M. Toward Understanding the origin and evolution of cellular organisms. *Protein Sci.* **28** (11), 1947–1951 (2019).
15. Kanehisa, M. & Goto, S. KEGG: Kyoto encyclopedia of genes and genomes. *Nucleic Acids Res.* **28** (1), 27–30 (2000).
16. Andrea, F. et al. STRING v9.1: protein-protein interaction networks, with increased coverage and integration. *Nucleic Acids Res.* ;**41**(D1). (2012).
17. Ideker, T. Cytoscape 2.8: new features for data integration and network visualization. *Bioinformatics* **27** (3), p431–p432 (2011).
18. Becht, E. et al. Dimensionality reduction for visualizing single-cell data using UMAP. *Springer Sci. Bus. Media LLC* 2019(1).
19. Aran, D. et al. Reference-based Analysis of Lung single-cell Sequencing Reveals a Transitional Profibrotic Macrophage. Nature Immunology.
20. Cai, Y. et al. A critical role of the IL-1β–IL-1R signaling pathway in skin inflammation and psoriasis pathogenesis. *J. Invest. Dermatology*. **139** (1), 146–156 (2019).
21. Church, L. D., Cook, Graham, P. & McDermott, M. F. Primer: inflammasomes and Interleukin 1β in inflammatory disorders. *Nat. Clin. Pract. Rheumatol.* (2008).
22. Chua, R. A., Arbiser, J. L., Chua, R. A. & Arbiser, J. L. The role of angiogenesis in the pathogenesis of psoriasis. *Autoimmunity* **42** (7), 574–579 (2009).
23. Heidenreich, R., Röcken, M. & Ghoreschi, K. Angiogenesis drives psoriasis pathogenesis. *Int. J. Exp. Pathol.* **90** (3), 232–248 (2009).
24. Yao Fang. *The Expression of STAT3 in Mouse Traumatic Skin Keratinocytes and the Effect of IL-22 on STAT3 Expression* (China Medical University, 2013).
25. Zeng, J. et al. Mannan-binding lectin exacerbates the severity of psoriasis by promoting plasmacytoid dendritic cell differentiation via the signal transducer and activator of transcription 3–interferon regulatory factor 8 axis. *J. Dermatol.* (5):49. (2022).
26. Gautier, G. et al. A type I interferon autocrine-paracrine loop is involved in Toll-like receptor-induced interleukin-12p70 secretion by dendritic cells. *J. Exp. Med.* **201** (9), 1435–1446 (2005).
27. Sano, S. et al. Stat3 links activated keratinocytes and immunocytes required for development of psoriasis in a novel Transgenic mouse model. *Nat. Med.* **11** (1), 43–49 (2005).
28. Zenewicz, L. A. IL-22 binding protein (IL-22BP) in the regulation of IL-22 biology. *Front. Immunol.* (2021).
29. Lu Yue, L. et al. Research progress on immune related genes in the pathogenesis of psoriasis. *Chin. J. Dermatology Venereol.* **35** (8), 5 (2021).
30. Gore, Y. et al. Macrophage migration inhibitory factor induces B cell survival by activation of a CD74-CD44 receptor complex. *J. Biol. Chem.* **283** (5), 2784–2792 (2008).
31. Bezdek, S. et al. Macrophage migration inhibitory factor (MIF) promotes TH17 cell-driven psoriasiform dermatitis. *Exp. Dermatol.* **26** (3), E60–E (2017).
32. Lanna, C. et al. Skin immunity and its dysregulation in psoriasis. *Cell. Cycle*. **18** (20), 2581–2589 (2019).
33. Li, Y. & Zhiqiang, Y. Interleukin-17 family and psoriasis. *China J. Lepr. Skin. Dis.* **33** (1), 3 (2017).
34. Johnston, A. et al. Keratinocyte overexpression of IL-17 C promotes psoriasiform skin inflammation. *J. Immunol.* **190** (5), 2252–2262 (2013).
35. Volari, I., Vii, M. & Prpi-Massari, L. The role of CD8 + T-Cells and their cytokines in the pathogenesis of psoriasis. *Acta Dermatovenerologica Croatica: ADC*. **27** (3), 159–162 (2019).
36. Schlapbach, C. et al. human t h 9 cells are skin-tropic and have autocrine and paracrine proinflammatory capacity. (2019).
37. Lowes, M. A. et al. Psoriasis vulgaris lesions contain discrete populations of Th1 and Th17 T cells. *J. Invest. Dermatology*. **128** (5), 1207–1211 (2008).
38. Song, Z. & Xing-Hua, G. Skin immune sentinels in health and disease. *Practical J. Clin. Med.* (2015).
39. Wang, H., Syrovets, T., Kess, D., Hainzl, B. B. & Lunov, H. Targeting NF-kappa B with a natural triterpenoid alleviates skin inflammation in a mouse model of psoriasis. *J. Immunol.* **183** (7), 4755 (2009).
40. Kanda, N. et al. Visfatin enhances CXCL8, CXCL10, and CCL20 production in human keratinocytes. *Endocrinology* (8):3155–3164. (2011).
41. Behfar, S., Hassanshahi, G., Nazari, A. & Khorramdelazad, H. A brief look at the role of monocyte chemoattractant protein-1 (CCL2) in the pathophysiology of psoriasis.
42. Sano, S. Stat3 links activated keratinocytes and immunocytes required for development of psoriasis in a novel Transgenic mouse model. *Nat. Med.* **11** (1), 43–49 (2005).

43. Bai, L. et al. STAT1 activation represses IL-22 gene expression and psoriasis pathogenesis. *Biochem. Biophys. Res. Commun.* **501** (2), 563–569 (2018).
44. Sutmuller, R., Garritsen, A. & Adema, G. J. Regulatory T cells and toll-like receptors: Regulating the regulators. *Ann. Rheum. Dis.* **66** (Suppl 3(Supplement 3), iii91–iii95 (2007).
45. Nakao, M., Sugaya, M., Fujita, H., Miyagaki, T. & Sato, S. TLR2 deficiency exacerbates Imiquimod-Induced Psoriasis-Like skin inflammation through decrease in regulatory T cells and impaired IL-10 production. *Int. J. Mol. Sci.* **21** (22), 8560 (2020).
46. Dombrowski, Y. et al. Cytosolic DNA triggers inflammasome activation in keratinocytes in psoriatic lesions. *Sci. Transl Med.* **3** (82), 82ra38 (2011).
47. Cai, Y. et al. Differential Developmental Requirement and Peripheral Regulation for Dermal Vγ4 and Vγ6T17 Cells in Health and Inflammation. Nature Publishing Group. 2014(1).
48. Vanbervliet, B. et al. Sequential involvement of CCR2 and CCR6 ligands for immature dendritic cell recruitment: possible role at inflamed epithelial surfaces. *Eur. J. Immunol.* (2002).
49. Frade, J. M. R., Mellado, M., Real, G. D. & Gutierrez-Ramos, J. C. Characterization of the CCR2 chemokine receptor: functional CCR2 receptor expression in B cells. *J. Immunol.* **159** (11), 5576 (1997).
50. Bernhagen, J. et al. MIF is a noncognate ligand of CXC chemokine receptors in inflammatory and atherogenic cell recruitment. *Nat. Med.* **13** (5), 587–596 (2007).
51. Leng, L. et al. MIF signal transduction initiated by binding to CD74. *J. Exp. Med.* **197** (11), 1467–1476 (2003).
52. Nobre, C. C. G., Araújo JMGd, F., Cobucci, T. A. A. M. & Fernandes, R. N. O. Macrophage migration inhibitory factor (MIF): biological activities and relation with Cancer. *Pathol. Oncol. Res.* **23** (2), 1–10 (2016).
53. Yu, X. et al. Macrophage migration inhibitory factor induces MMP-9 expression in macrophages via the MEK-ERK MAP kinase pathway. *J. Interferon Cytokine Res.* **27** (2), 103–109 (2007).
54. O'Shea, J. J., Holland, S. M. & Staudt, L. M. JAKs and stats in immunity, immunodeficiency, and cancer. *N Engl. J. Med.* **368** (2), 161–170 (2013).
55. Bernard, F. X. et al. Keratinocytes under fire of Proinflammatory cytokines: Bona Fide innate immune cells involved in the physiopathology of chronic atopic dermatitis and psoriasis. *J. Allergy (Cairo)*. **2012**, 718725 (2012).
56. Lai, Y. et al. Commensal bacteria regulate Toll-like receptor 3-dependent inflammation after skin injury. *Nat. Med.* **15** (12), 1377–1382 (2009).

Acknowledgements

We extend our gratitude to all the contributors of data utilized in this study. Our appreciation also extends to the editors and anonymous reviewers whose insightful suggestions greatly enriched the manuscript. We would like to thank all the donors who contributed samples.

Author contributions

TY and LM designed the study. TY led the data collection, analysis interpretation, and manuscript writing. LM and TZ revised the manuscript and provided administrative support. All authors made significant contributions to the article and approved the version submitted for publication.

Funding

The research was supported by the National Natural Science Foundation of China (32060145, 32060300 and 31860308). The funders had no role in the study design, data collection and analysis, decision to publish, or preparation of the manuscript.

Declarations

Competing interests

The authors declare no competing interests.

Consent for publication

Not applicable.

Institutional review board statement

The study was conducted in accordance with the Declaration of Helsinki and approved by the Ethics Committee from The First Affiliated Hospital of Shihezi University, China (Approval Number: KJ2024-293-02).

Informed consent

Informed consent was obtained from all subjects involved in the study.

Additional information

Supplementary Information The online version contains supplementary material available at https://doi.org/10.1038/s41598-025-02822-1.

Correspondence and requests for materials should be addressed to T.Z. or L.M.